Re: (nhess-2017-336) Assessment of peak tsunami amplitude associated with a great earthquake occurring along the southernmost Ryukyu subduction zone for Taiwan region *by* Yu-Sheng Sun, Po-Fei Chen, Chien-Chih Chen, Ya-Ting Lee, Kuo-Fong Ma, and Tso-Ren Wu

Dear Prof. Lionello,

Thank you for reviewing this paper. We have made the revision to our manuscript intensively and reply the comments from reviewers carefully for your further consideration on the publication in Natural Hazards and Earth System Sciences (***NHESS***).

The authors highly appreciate the support of publication in ***NHESS*** from the reviewers and their helpful suggestion as well. We have made substantive modifications according to their suggestion and the **English editing by Springer Nature**. The annotated responses to the reviewers' comments and the details about our changes in the revised version of our manuscript are made accordingly in the files. Attached please also find the electronic files of the revised manuscript for your further consideration of publication in ***NHESS***. In the revised version, all modifications were marked in red for your reference. Any problem raised please let me know. Thank you very much.

With Best Regards,
Yu-Sheng Sun

Nature Research Editing Service Certification

This document certifies that the manuscript listed below was edited for proper English language, grammar, punctuation, spelling, and overall style by one or more of the highly qualified native English speaking editors at American Journal Experts.

This certificate may be verified at www.aje.com/certificate. This document certifies that the manuscript listed above was edited for proper English language, grammar, punctuation, spelling, and overall style by one or more of the highly qualified native English speaking editors at American Journal Experts. Neither the research content nor the authors' intentions were altered in any way during the editing process. Documents receiving this certification should be English-ready for publication; however, the author has the ability to accept or reject our suggestions and changes. To verify the final AJE edited version, please visit our verification page. If you have any questions or concerns about this edited document, please contact American Journal Experts at support@aje.com.

Manuscript title: Assessment of peak tsunami amplitude associated with a great earthquake occurring along the southernmost Ryukyu subduction zone for Taiwan region

Authors: Yu-Sheng Sun, Po-Fei Chen, Chien-Chih Chen, Ya-Ting Lee, Kuo-Fong Ma, Tso-Ren Wu

Key: 9C78-0668-60FF-F9C0-81B7

This certificate may be verified at **secure.authorservices.springernature.com/certificate/verify**.

Response (in black) to the comments of Reviewers (in blue)

Reviewer #1:

In Table 1, if at hand please add the water depth at the tide gauges as they appear in the computational mesh. This value is needed to reproduce the results.
We have added the values of water depth in Table 1. [Pages 26-27]

Reviewer #2:

Page 1, Abstract, line 9. I suggest to change, "tsunami earthquakes" by "tsunamigenic earthquakes", to avoid any confusion with the "tsunami-earthquake" itself. I assume authors refer to any kind of earthquake that generates a tsunami (e.g. regular earthquakes, tsunami-earthquakes, etc.).
We have done it. [Page 1, line 12]

Page 3, line 16. Please, insert "vary" after (Delta_sigma).
We have done it. [Page 4, line 2]

Page 3, line 21. Change "is" by " are".
We have done it. [Page 4, line 7]

Page 3, line 22. I suggest to change "a definite" by "the assumed".
We have done it. [Page 4, line 8]

Page 3, line 27. I think a word is missing in the sentence "..can be transformed magnitude Mw", so, I will suggest, "...can be transformed to magnitude Mw".
Thank you. We have done it. [Page 4, lines 14-15]
According to the suggestion of English editing, it was written "…can be transformed into the magnitude M_w".

Page 4, line 2. Please, insert the physical unit in the value of M0, I guess it is [dyne-cm].
We have done it. [Page 4, line 17]

Page 4, line 6. For better description, complete the word "temporal" by "spatio-temporal".
We have done it. [Page 4, line 21]

Page 4, line 13. I suggest to insert "The" before "k-2".

We have done it. [Page 5, line 2]

Page 4, line 15. For a better reading, I will suggest to change "self-similar introducing the...", "self similarity introduced the...".

We have done it. [Page 5, lines 3-4]

According to the suggestion of English editing, we modified the sentence.

Page 4, line 20. I think instead of "convolution in the Fourier domain" it should be, "multiplication in the Fourier domain", because the 2D Fourier spectrum of the random realization of slip is multiplied by k-2 in the Fourier domain beyond some characteristic wavelength.

We have done it. [Page 5, line 9]

In Lavallée and Archuleta, (2003) and Lavallée et al. (2006), they both used “convolution” to describe this calculation, but we agree that using multiplication is more appropriate.

Page 4, line 25. I suggest to replace "4" by "four".

We have done it. [Page 5, line 14]

Page 5, line 6. The "convoluting" operation is not correct. I will suggest to write something like, "by imposing a self-similar characteristic...".

We have done it. [Page 5, lines 24-25]

Page 5, line 8. Correct "gird" by "grid".

We have done it. [Page 5, lines 26-27]

Page 5, line 10. I will suggest to insert "shown in" before "Figure 1a".

We have done it. [Page 5, line 29]

Page 5, line 13. To complete the idea, I suggest to insert "faulting" before "mechanism".

We have done it. [Page 6, line 3]

Page 5, line 13-14. I think the sentence "In addition, the inversed slip distribution in study region is lack to do the analysis of Levy PDF" could be better executed. For instance, "There are not inverted slip models of past earthquakes in the study area to do the analysis of Levy PDF parameters.", or something like that.

We have done it. [Page 6, lines 4-5]

Page 5, line 23. I will suggest to insert "the plate interface" before "..is locked..".

We have done it. [Page 6, line 17]

Page 5, line 24. To complete the idea, I suggest to add "over the whole fault plane" after "...uniform slip distribution.".

We have done it. [Page 6, lines 21-22]

Page 7, line 27. Please, provide physical units to 1.024, m ?

We have done it. [Page 8, line 30]

Page 9, line 5. It is just a suggestion, but to better precise the idea, I suggest to modify the phrase "...is parallel the subduction zone.." by "..is parallel to the trench axis of the subduction zone", or something like that.

We have done it. [Page 10, lines 21-22]

Page 9, line 6. Insert "along" before "these".

We have done it. [Page 10, line 26]

Page 9, Paragraph 2 and 3. To help the reader, I suggest to label the four NPPs (Nuclear Power Plants) in Figure 5, map on the right. The NPPs are labeled in Figure 2, but because authors discuss the NPP3, NPP2, etc, with respect to the PTA at different locations along the coast of Taiwan in Figure 5 again, it will be useful to see the label of each NPP in this figure.

We have done it. [Page 24]

Page 9, line 6. Wildest ?, or should it be "widest" ?. Please, clarify.

We have done it. [Page 13, line 6]

Thank you. I find this word on page 11, the section of Conclusion.

Page 9, line 7. Please, provide physical units to 1.63, m ?.

We have done it. [Page 13, line 7]

Figures

Figure 2. I will suggest to complement "(5x5 km2)", by "(5x5 km2 grid size)".

We have done it. [Page 19, line 5]

Figure 5. See my comments above (Page 9, Paragraph 2 and 3). It will be useful to label each NPP in the map on the right. Please, describe a little bit the map on the right in the caption. For instance, "Map of Taiwan with station locations and four NPP (yellow squares)."

We have done it. [Page 24]

p.s.

Figure 1.

We have changed “Fit:” to “fit”.

Figure 2.

We modified the resolution.

Figure 4.

We changed “hour” to “hours” for x-label.

Figure 6.

We changed “hight” to “height” for y-label.

Assessment of the peak tsunami amplitude associated with a great earthquake occurring along the southernmost Ryukyu subduction zone ~~for~~in the region of Taiwan ~~region~~

Yu-Sheng Sun[1], Po-Fei Chen[1], Chien-Chih Chen[1,2], Ya-Ting Lee[1,2], Kuo-Fong Ma[1,2] and Tso-Ren Wu[2,3]

[1]Department of Earth Sciences, National Central University, Taoyuan City 32001, Taiwan ~~320~~, R.O.C.
~~[2]Graduate~~[2]Earthquake-Disaster & Risk Evaluation and Management Center, National Central University, Taoyuan City 32001, Taiwan, R.O.C.
[3]Graduate Institute of Hydrological and Oceanic Sciences, National Central University, Taoyuan City 32001, Taiwan ~~320~~, R.O.C.

Correspondence to: Yu-Sheng Sun (shengfantasy@gmail.com)

Abstract. The southernmost portion of the Ryukyu Trench ~~closed to~~ near the island of Taiwan ~~island is a potential region to generate 7.5 to 8.7 tsunami~~potentially generates tsunamigenic earthquakes ~~by~~with magnitudes from 7.5 to 8.7 through shallow rupture. The fault model for this potential region dips 10° northward with a rupture length of 120 km and a width of 70 km. ~~The~~An earthquake magnitude of Mw 8.15 is estimated by the fault geometry ~~is Mw 8.15~~ with ~~8.25 m~~an average slip of 8.25 m as a ~~constrain of~~constraint on the earthquake scenario. ~~The heterogeneous~~Heterogeneous slip distributions over the rupture surface are generated by a stochastic slip model, which represents that the slip spectrum ~~with~~ decays according to k^{-2} ~~decay~~ in ~~wave number~~the wavenumber domain~~, and they~~. These synthetic slip distributions are consistent with the above mentioned identical seismic conditions. The results from tsunami ~~simulation~~simulations illustrate that the propagation of tsunami waves and the peak wave heights largely vary in response to the slip distribution. ~~The~~ Changes in the wave phase ~~changing is~~are possible as the waves propagate, even under the same seismic conditions. The tsunami energy path ~~is~~ not only ~~following~~follows the bathymetry but also ~~depending~~depends on the slip distribution. The probabilistic distributions of the peak tsunami amplitude calculated by 100 different slip patterns from 30 recording stations reveal that the uncertainty decreases with increasing distance from the tsunami source. The highest wave amplitude for 30 recording points is 7.32 m at Hualien for 100 different slips. ~~Comparing~~Compared with the stochastic ~~slips,~~slip distributions, the uniform slip distribution will be extremely underestimated, especially in the near field. In general, the uniform slip assumption ~~only~~ represents only the average phenomenon ~~so that it~~and will consequently ignore the possibility of tsunami ~~wave~~waves. These results indicate that considering ~~effect~~the effects of heterogeneous slip ~~distribution~~distributions is necessary for assessing tsunami ~~hazard and that can~~hazards to provide ~~more~~additional information about tsunami ~~uncertainty for~~uncertainties and facilitate a more comprehensive estimation.

1 Introduction

Almost all destructive tsunamis are generated by shallow earthquakes that occur ~~at~~within subduction ~~zone. There were recently~~zones. Numerous destructive tsunami events~~:~~, including the ~~2004,~~ Mw 9.1~~,~~ Sumatra earthquake in 2004 (Lay et al., 2005), the ~~2010,~~ Mw 8.8~~,~~ Chile earthquake in 2010 (Lay et al., 2010; Fritz et al., 2011) and the ~~2011,~~ Mw 9.0~~,~~ Tohoku earthquake in 2011 (Goda et al., 2015; Goda and Song, 2016~~);~~), all of ~~them~~which occurred ~~at~~in subduction ~~zone.~~zones, have occurred recently. The island of Taiwan, which is located at the convergent boundary between the Philippine Sea Plate and the Eurasian Plate ~~is possibly threatened from~~, is constantly under the possible threat of a tsunami. The convergence rate in this area is approximately 80-85 mm/yr (Seno et al., 1993; Yu et al., 1997; Sella et al., 2002; Hsu et al., 2009; Hsu et al., 2012). Thus, earthquakes occur frequently in and around Taiwan. The shallow earthquakes that occur in the Manila Trench to the south and the Ryukyu Trench to the northeast are particularly tsunamigenic~~. Also, the~~, and earthquakes ~~in~~ occur more actively in the southernmost Ryukyu Trench ~~is more active~~ than ~~north~~in the northern Manila Trench (Wu et al., 2013). The most well-known historic tsunami events that have occurred in ~~northeast~~northeastern Taiwan are the 1867 Keelung earthquake (Mw 7.0) (Tsai, 1985; Ma and Lee, 1997; Cheng et al., 2016; Yu et al., 2016) and the 1771 Yaeyama (Japan) earthquake (M_w~8) (Nakamura, 2009a). ~~The~~Accordingly, these historic ~~recording demonstrates~~recordings demonstrate that Taiwan ~~island has the~~is under a potential ~~of~~ tsunami threat. Furthermore, the 2011 Tohoku earthquake induced a powerful tsunami that destroyed coastal areas and caused nuclear accidents (Mimura et al., 2011). ~~There~~As there are four nuclear power plants along the coast ~~on~~of Taiwan~~ island so that~~, it is necessary to carefully estimate the tsunami hazard ~~and~~in addition the hazards of compound disasters.

Probabilistic tsunami hazard analysis (PTHA) is a modification of probabilistic seismic hazard analysis (PSHA) (Cornell, 1968; SSHAC, 1997), and it is intended to forecast ~~as comprehensively as possible~~ the probability of tsunami hazards for a given region~~. Considering tsunamis triggered by earthquakes, the~~ as comprehensively as possible. The recurrence rates of earthquakes have typically been estimated using the Gutenberg–Richter relationship (Gutenberg and Richter, 1944) for a defined source region~~.~~ in consideration of tsunamis triggered by earthquakes. The assessment of the wave ~~heights~~height is one of the primary differences between PTHA and PSHA. PSHA assesses the ground motion based on empirical attenuation relationships (Wang et al., 2016~~).~~), while PTHA assesses tsunami wave heights using empirical approaches or tsunami simulations (Geist, 2002; Geist and Parsons, 2006; Geist and Parsons, 2009). Geist and Parsons (2006) ~~mentions~~mentioned that the tsunami wave height follows a definable frequency-size distribution over a sufficiently long ~~amount~~period of time ~~at~~within a given coastal region (Soloviev, 1969; Houston et al., 1977; Horikawa and Shuto, 1983; Burroughs and Tebbens, 2005). This method is of great use in establishing the tsunami probability for ~~regions~~a region if there is an extensive catalog of observed tsunami wave heights. ~~Given~~However, given the wide distribution of global tsunamigenic earthquakes within seafloor regions ~~at~~throughout subduction zones, the tsunami records obtained from coastal gauges or/and ocean buoys are too sparse to comprehensively assess the associated hazards~~ comprehensively~~, and the recording time since their deployment is too short to enable a study of the recurrence intervals of tsunamis/earthquakes. ~~The~~ Consequently, because the existing tsunami catalogue is limited~~ so that the simulation is~~, simulations represent an effective approach. Conventional tsunami simulation adopts a simple source approximation and applies elastic dislocation theory to calculate the deformation of the seafloor surface assuming a uniform slip over the entire fault surface (Okada, 1985; Okal, 1982). However, the ~~complexity~~complexities of earthquake ~~ruptures plays~~rupture processes play a substantial role in ~~tsunami~~the generation of tsunamis. Conventional approaches are therefore unable to capture various features of short-wavelength tsunamis in the near field (Geist, 2002; Geist and Parsons, 2009). ~~Previous~~The results of previous studies that ~~simulate~~simulated tsunamis ~~resulting~~originating from historical earthquakes around Taiwan (Ma and Lee, 1997; Wu et al., 2008) using uniform slip models ~~agree~~agreed only with long-wavelength observations. For the purposes of hazard mitigation, it is critical ~~that~~to predict the amplitudes of tsunamis ~~are predicted~~ along various ~~coasts~~coastlines for a given earthquake as accurately as possible. To make such predictions, the effects of the rupture complexity must be taken into consideration. Recent developments in PTHA have included the adoption of stochastic slip distributions of earthquakes to determine the overall probability of particular tsunami heights~~.~~ (Geist and Parsons, 2006, 2009). ~~That method can be~~The adoption of stochastic slip distributions is able to quantify the variations ~~for a~~in reasonable ~~estimation in evaluating~~evaluations of the ~~probability~~probabilities of specified tsunami heights at individual locations ~~that result~~resulting from a specific fault.

In this study, we assess ~~tsunami~~the heights of tsunamis along the ~~coasts~~coastline of Taiwan ~~that is caused~~generated by the potential tsunamigenic zone at the southernmost end of the Ryukyu subduction zone. This potential zone is located close to Taiwan, and at least ten earthquakes (M_w>7) have occurred over the past 100 years (Hsu et al., 2012~~). The~~), the largest ~~one is~~of which was the Mw 7.7 in 1920 (Theunissen et al., 2010). For this area, the plausible magnitude of greatest earthquake ~~was~~is determined ~~to a~~within the range between 7.5 and 8.7 (M_w) (Hsu et al., 2012). The fault zone is bounded by the Longitudinal Valley Fault to the west and the Gagua Ridge to the east (Hsu et al., 2012). This ~~defined~~ fault geometry with a defined rupture length and width ~~was~~is employed herein, and an earthquake with a magnitude of 8.15 is used in the tsunami ~~simulations~~simulation. The stochastic slip model is invoked to describe the uncertainty ~~of~~in the rupture pattern over the fault plane to enable a more realistic assessment of the tsunami probability.

2 ~~Great earthquake~~Earthquake scenario and tsunami simulation

2.1 Assessment of Seismic Parameters

The ~~estimating~~ estimated maximum magnitude of ~~the maximum~~a possible earthquake scenario is essential for establishing the fundamental seismic ~~condition~~conditions of the tsunami simulation. ~~This~~The scenario~~,~~ of a potential rupture fault~~,~~ extending to a depth of 13 km proposed by Hsu et al. (2012) occurs along the southernmost Ryukyu trench with a rupture length of 120 km, a width of 70 km and a dip of 10°~~ and extends to a depth of 13 km.~~. Kanamori and Anderson (1975) investigated the relation between the rupture area and moment~~, which~~ and revealed that ~~the~~ most of the average stress drops ($\Delta\sigma$) vary between 10 ~~to~~and 100 bars. The average stress ~~drops~~drop for ~~the~~ most interplate earthquakes ~~are around~~is approximately 30 bars~~ so that~~, and thus, we set an average stress drop of 30 bars. ~~According to the~~The stress drop and seismic moment (M_0) ~~relations in~~relation along a dip slip ~~faults~~fault is described as follows (Kanamori and Anderson, 1975):

$$M_0 = \frac{\pi(\lambda+2\mu)}{4(\lambda+\mu)}\Delta\sigma W^2 L \qquad (1)$$

where W and L ~~is~~are the width and length of the rupture plane, respectively. We can obtain the moment for this scenario under ~~the~~an average stress drop of 30 bars ~~and~~ with ~~a definite~~the assumed rupture geometry. In Eq. (1), μ ~~is~~denotes the rigidity and λ is the Lamè parameter. We assume that the crust is elastic and homogeneous. Hence, μ ~~=~~ = λ ~~=~~ = 30 GPa (Fowler, 2004; Piombo et al, 2007). Additionally, the seismic moment can be ~~presented~~represented by the rupture area and average slip as ~~below~~follows (Lay and Wallace, 1995):

$$M_0 = \mu A \bar{D} \qquad (2)$$

~~The~~ Moreover, the seismic moment~~, moreover,~~ is dependent on the rupture area (A) and average slip ($\bar{D}$~~) so that~~); thus, the average slip can be estimated by ~~following~~ Eq. (2~~)~~), and it is calculated to be 8.25 m. Then, the seismic moment can be transformed into the magnitude M_w by the following (Hanks and Kanamori, 1979~~)~~):

$$M_w = \left(\frac{\log M_0}{1.5}\right) - 10.73 \qquad (3)$$

Therefore, the maximum possible earthquake magnitude is M_w 8.15 (M_0 ~~=~~ = 2.07×10^{28} dyne-cm).

2.2 Stochastic Slip Model

The rupture process of an earthquake is extremely complex. ~~The seismic~~Seismic inversion results reveal that the slip distribution of a rupture ~~is~~has a heterogeneous ~~with~~ spatio-temporal development. ~~Using~~Consequently, using a simplified uniform slip distribution to simulate a tsunami ~~only~~ captures only the long-wavelength portion of the tsunami ~~fields~~field (Geist and Dmowska, 1999). In addition, the temporal description of the seismic rupture process can be ignored because the propagation velocity of the tsunami ~~waves~~wave is substantially slower than the seismic rupture velocity (Dean and Dalrymple, 1991; Ma et al., 1991; Wang and Liu, 2006). Andrews (1980) showed that the static slip distribution is directly related to stress changes and that the spectrum of the slip distribution is proportional to k^{-2} decay in the wavenumber domain:

$$\left|F_{s,t}\left[D_{x,y}\right]\right| \propto k^{-2} \qquad (4)$$

where $D_{x,y}$ is the slip distribution over a 2D lattice, $F_{s,t}$ is the 2D Fourier transform, and $k=\sqrt{k_x^2+k_y^2}$ is the radial wavenumber. The k^{-2} power law ~~illustrates~~indicates that the slip distribution has self-similar characteristics ~~and from the fractal perspective~~; moreover, this characteristic can also ~~can~~ be demonstrated from a fractal perspective (Tsai, 1997). Based on self-similarity, Herrero and Bernard (1994) ~~based on self-similar introducing~~introduced the k-square model, which leads to the ω-square model (Aki, 1967). The slip spectrum follows k^{-2} decay beyond the corner radial wavenumber~~, –~~ (k_c~~,~~), which is proportional to $1/L_c$. The L_c depends on the characteristic rupture dimension (Geist, 2002).

The heterogeneous slip distribution is proportional to k^{-2} and is similar to ~~a~~ fractional Brownian motion as a stochastic process (Tsai, 1997). The stochastic slip distribution can be described by ~~convolution~~multiplication in the Fourier domain~~,~~:

$$D_{x,y} \propto F_{x,y}^{-1}\left[F_{s,t}\left[X_{x,y}\right]\times k^{-2}\right] \qquad (5)$$

where $X_{x,y}$ is a random variable for the spatial distribution~~; moreover, it makes~~ that randomizes the phase ~~random.~~, and $F_{x,y}^{-1}$ is the inverse 2D Fourier transform. The random distribution~~,~~ of X, which is best described by a non-Gaussian distribution, especially by a Lèvy distribution, can be calculated by reversing Eq. (5) (Lavallée and Archuleta, 2003; Lavallée et al., 2006). The Lèvy distribution can be described by ~~4~~four parameters, namely, α, β, γ and μ_L~~.~~, as ~~below~~follows:

$$\varphi(t)=\begin{cases}\exp\left(-\gamma^{\alpha}|t|^{\alpha}\left[1+i\beta\,\mathrm{sign}(t)\tan\frac{\pi\alpha}{2}\left(|\gamma t|^{1-\alpha}-1\right)\right]+i\mu_L t\right), & \alpha\neq 1\\ \exp\left(-\gamma|t|\left[1+i\beta\frac{2}{\pi}\mathrm{sign}(t)\left(\ln|t|+\ln\gamma\right)\right]+i\mu_L t\right), & \alpha=1\end{cases} \qquad (6)$$

The parameter α, $0<\alpha\le 2$, affects the falloff rate of the probability density function (PDF) for the tail. The parameter β, $-1\le\beta\le 1$, controls the skewness of the PDF~~. The~~, and the parameter γ, $\gamma>0$, controls the width of the PDF. The parameter μ_L, $-\infty<\mu_L<\infty$, is related to the location of the PDF. The Lèvy distribution is ~~good to describe~~effective at describing the distribution of a random variable, i.e., X, from real earthquake events, ~~which implies~~ implying that the slip distribution without self-~~similar characteristic~~similarity has a heavy tail behavior (Lavallée et al., 2006). ~~From the~~Based on experiments of generating stochastic slip ~~distribution, the~~ distributions, this heavy tail behavior affects the intensity of an extreme value (Lavallée and Archuleta, 2003).

The stochastic slip distribution is generated by a 2D ~~spatial~~spatially random distribution ~~with convoluting~~by imposing a self-similar characteristic beyond the corner radial wavenumber, ~~constraining~~which is constrained by the rupture dimension, in the wavenumber domain. In this study, the potential rupture fault is divided into 5×5 km^2 subfaults. The ~~number~~grid is composed of ~~gird mesh is~~ 24×14 ~~which are~~meshes along the strike and dip directions, respectively. The ~~spatial random variable~~ produced variable with a spatially random distribution adopts the Lèvy distribution (α=1.51, β=0.2, γ=28.3, μ_L=-0.9~~)~~), which is the dip slip result from Lavallée et al. (2006) as ~~Figure~~ shown in Fig. 1a. In Lavallée et al. (2006), the slip distribution of the Northridge earthquake ~~had been~~was divided into the dip~~-~~-slip and strike~~-~~-slip directions, and they were calculated by an inverse 2D stochastic model to obtain the values of the Lèvy PDF. The values of the Lèvy PDF, which are mentioned above are ~~given over to~~ indicative of the result of dip~~-~~-slip direction. The Northridge earthquake is a thrust earthquake (Davis, 1994~~) so that~~), and thus, it ~~roughly~~ has ~~similar~~a faulting mechanism ~~with~~ that is approximately similar to our scenario fault model. ~~In addition, the inversed~~There are no inverted slip ~~distribution in~~models of past earthquakes in the study ~~region is lack~~area to ~~do the~~conduct an analysis of ~~Lèvy~~the Levy PDF~~. Therefore~~ parameters; therefore, the ~~value of~~ Lèvy distribution in Lavallée et al. (2006) is adopted in this study. ~~In~~From the perspective of mathematical ~~operation~~operations, the slip distribution in Eq. (5) ~~is~~represents a ~~kind of~~ filtered random distribution. However, for consistency with the physical behavior over the rupture surface ~~supposed~~suggested by the results of the inverse ~~method, the~~modeling, truncation ~~has to~~of the Lèvy distribution must be ~~applied to the Lèvy distribution~~performed to constrain the extreme slip value. The synthetic slip distribution (Fig. 1b) produced by ~~spatial~~the spatially random distribution in ~~Figure~~Fig. 1a is heterogeneous, and its power spectrum obeys a *k*-square model at high ~~wavenumber~~wavenumbers (Fig. 1c). The average slip of this synthetic slip distribution is 8.25 m, ~~which represents~~ indicating that the earthquake energy ~~keeping a~~is constant as ~~estimating~~estimated above, and the maximum slip is 31.02 m. ~~The 100~~One hundred different slip distributions are produced for the tsunami simulation~~. They represent~~ representing the uncertainty ~~of~~in the results ~~of~~ associated with complex rupture ~~process~~processes. In the 100 sets of results, the maximum slip range is between 20.17 ~~to~~and 37.97 m. ~~There are no smooth process and extra~~Smooth processes are not included, nor are additional regional ~~constrain~~constraints for the slip distribution. There are two reasons for this application. The first is that we do not have information ~~for~~regarding where the plate interface is locked or the ~~location~~locations of ~~asperity~~asperities often ~~repeats~~repeat in historical ~~event~~events. The second is that ~~there are~~ some studies ~~present~~reported that the ~~asperity expanding~~asperities extend to the boundary of the fault model (Ide et al., 2011; Lay et al., 2011; Shao et al., 2011; Yue and Lay, 2011). According to these reasons, we do not ~~prefer to~~ apply any ~~extra constraint~~additional constraints for stochastic slip distributions. ~~By same token~~Similarly, the uniform slip case ~~is~~constitutes a complete uniform slip distribution~~.~~ over the whole fault plane. Figure 1b and 1d ~~are~~demonstrate the stochastic distribution of the scenario source models causing the maximum and minimum wave ~~height~~heights, respectively, at ~~the~~ recording station 26 (Hualien) (Fig. 2). Both patterns affecting the propagation will ~~show at~~ be discussed in Sect. 3.1.

2.3 Numerical Tsunami Simulation

Figure 2 shows the computational domain, recording stations and fault model. The potential rupture fault is divided into 5×5 km^2 subfaults, and the stochastic slip distribution model is applied to determine the amount of discrete slip on each subfault. Vertical seafloor displacements caused by slip along the rupture ~~slip~~plane are calculated using elastic dislocation theory (Okada, 1985). The Cornell ~~Multigrid~~Multi-grid Coupled Tsunami ~~Model~~model (COMCOT) is used to perform the tsunami simulations. COMCOT is capable of efficiently studying the entire life-span of a tsunami, including its generation, propagation, runup and inundation (Wang, 2009~~). It~~), and it has been widely used in studying many historical tsunami events, such as the 1960 Chilean tsunami (Liu et al., 1995), 1992 Flores Islands tsunami (Liu et al., 1995), 2003 Algeria tsunami (Wang and Liu, 2005), 2004 Indian Ocean tsunami (Wang and Liu, 2006, 2007), and 2006 Ping-Tung tsunami, Taiwan (Wu, et al., 2008; Chen, et al., 2008). COMCOT solves ~~the~~ linear or nonlinear shallow water equations for spherical or Cartesian coordinates using the finite difference method. With ~~the~~a flexible nested grid system, it can properly ~~exhibit~~guarantee both the efficiency and the accuracy from the near-coastal region to the far-field region. Two grid layers are used to simulate the propagation of tsunamis. The Manning coefficient is 0.013 in this study to assume a sandy sea bottom (Wu~~,~~ et al., 2008). The bathymetry adopted ~~NOAA's (~~open data from the National Oceanic and Atmospheric Administration~~) open data which~~ (NOAA) that can be download from https://maps.ngdc.noaa.gov/viewers/wcs-client/ (Amante and Eakins, 2009). The resolution of the outer layer is 4 minutes for the solution of the linear shallow water equation, and the resolution of the inner layer is 1 minute for the solution of the nonlinear form of the shallow water equation. There are 30 recording stations ~~which refer~~referring to the positions of tidal gauges maintained by the Central Weather Bureau (CWB) along the ~~coasts~~coastlines of Taiwan and the outlying islands. The CWB website ~~of CWB~~ presents the ~~location~~locations of the tide stations (http://e-service.cwb.gov.tw/HistoryDataQuery/index.jsp and http://www.cwb.gov.tw/V7e/climate/marine_stat/tide.htm~~.~~). These locations are shifted slightly to the ~~node of~~ grid ~~in order~~nodes to ~~record~~ accurately~~.~~ record the data. Table 1 presents the locations ~~of~~and water depths of the recording stations in the computational mesh.

3 The effect of heterogeneous slip on ~~the~~ tsunamis

The stochastic slip model produces different slip distributions with the same fault geometry~~,~~ in addition to a constant average slip and a constant seismic moment. The model is used to describe the heterogeneous slip pattern of an earthquake and to further examine its effect on the tsunamis ~~occurring at~~originating from the southernmost end of the Ryukyu subduction zone adjacent to Taiwan. According to the previous sections, the maximum possible earthquake magnitude is determined to be M_w 8.15 with ~~8.25 m~~an average slip of 8.25 m. Furthermore, the uniform slip distribution on the rupture plane is also used to simulate tsunami ~~for discussing~~to facilitate a discussion of the ~~different~~difference between the effects of uniform and heterogeneous slip on ~~the~~ tsunamis.

3.1 Initial water elevation and energy propagation

The static vertical displacement of the ocean floor is ~~modelled~~modeled using ~~the~~ elastic dislocation theory (Okada, 1985) ~~and considered~~with a static slip distribution. The vertical seafloor displacement is ~~used to be~~modeled as the initial water level, and the horizontal component of the seabed displacement is not included in the simulation. Figure 3a shows the initial water elevations produced by a uniform slip distribution, and ~~Figure~~Fig. 3b ~~is its~~exhibits the maximum free-surface elevation during the propagation. Figure 3c and 3e ~~are~~demonstrate the initial water elevations produced by the stochastic slip distributions (Fig. 1b and 1d). The initial water elevation ~~by~~with a uniform slip distribution is simple and smooth, but ~~for the~~those with stochastic slip models are more complex and ~~more~~relatively heterogeneous. Nonuniform slip causes an apparent change in the wavelength distribution of the initial free-surface elevation (i.e., the potential energy distribution), which affects the path of energy propagation. In the uniform slip scenario, the maximum free-surface elevation pattern is ~~clear~~straightforward and clearly controlled by the topography. However, many strong and seemingly chaotic paths of wave energy appear in the nonuniform slip scenarios, and the ~~ocean~~ free-surface field ~~has more~~exhibits additional uncertainties in terms of the flow. In ~~Figure~~Fig. 3b, the maximum free-surface elevation mainly ~~travels~~propagates toward two places where the seafloor ~~elevation~~bathymetry becomes shallower~~,~~ relative to the deep areas northeast of Taiwan as ~~bathymetry~~shown in Fig. 2. Although the propagation ~~by~~ paths due to the nonuniform slip distributions (Fig. 3d and 3f) also ~~has~~have the same characteristics, it is notable that the paths followed by the wave energy differ~~, which depends~~ depending on the rupture pattern. ~~At~~To the northeast of Taiwan in ~~Figure~~Fig. 3f, there is a strong wave path connecting the two higher~~-~~-elevation ~~part~~areas of bathymetry. However, this behavior ~~does~~is not ~~occur~~observed in ~~Figure~~Fig. 3b and 3d. ~~Besides that, at the footwall side~~In addition, the maximum elevation ~~of Figure~~on the footwall in Fig. 3d is higher than ~~Figure~~that in Fig. 3f. In ~~Figure~~Fig. 3b, the high elevation ~~only~~ appears only along the coast ~~at~~on the footwall side. These results indicate that the wave energy variation depends on the rupture pattern, thereby causing differences in the wave paths and ~~leads~~leading to ~~totally~~completely different tsunami amplitudes.

3.2 Wave ~~characteristic~~characteristics

~~There are 30~~Thirty stations located along the ~~coasts~~coastlines are available for recording the ~~motion~~amplitude of ~~sea level.~~the tsunami wave height. Relative to the other stations, ~~the station~~stations 25 (Shihti), 26 (Hualien) and 27 (Suao) are situated near the potential rupture fault, and they have high wave ~~amplitude~~amplitudes and enormous ~~variation~~variations in the tsunami ~~simulation~~simulations of 100 different slip distributions~~ so that~~; consequently, the time series of the wave heights at these stations are shown as an example (Fig. 4). The ~~varied wavelength~~variability in the distribution of the initial free-surface elevation results in substantial phase changes and different wave heights. ~~It's~~It is worth noting that the average of the disordered and chaotic time series produced by the 100 different slip distributions is almost identical to the results ~~from~~of the time series produced by the uniform case. This implies that the uniform ~~case~~slip distribution simply represents an average result and that it cannot represent all of the possible situations.

According to the statistical results from 100 different slip patterns (Table 1) for 30 stations, Hualien station has the maximum wave amplitude~~,~~ of 7.32 m, and its maximum wave amplitude interval ~~is~~ranges from 1.87 to 7.32 m~~. It is~~, which constitutes the widest interval for any recording site, and the standard deviation of this distribution is 1.024 m. These findings indicate that Hualien station has a high uncertainty in this scenario setting. However, the maximum wave amplitudes from the uniform slip distribution are relatively lower than those from the stochastic results. Following the above ~~lecture~~findings, we need to

~~rethink about that the estimation of~~consider whether the estimations from the uniform slip case ~~is available~~are appropriate for hazard analysis ~~or not, even only~~by focusing on the maximum wave amplitude issue.

3.3 The peak tsunami amplitude probability

According to the results of our simulations, we ~~calculated~~calculate the probability of the peak/maximum tsunami ~~amplitudes~~amplitude (PTA) at each recording station as shown in ~~Figure 5 by~~the histogram of Fig. 5. To verify the representativeness of the PTA probability distributions, another 100 sets of different slip distributions ~~had been~~are produced ~~with~~ and simulated under the same seismic conditions ~~and simulated.~~. In ~~Figure~~Fig. 5, the shapes of the PTA distributions from another 100 sets~~,~~ (black lines~~,~~) are similar to the shapes of the histograms~~,~~ from the first 100 sets. ~~This~~These results verify the representativeness of the PTA probability distributions ~~in~~produced from 100 sets of slip distributions. This test also reinforces the reproducibility of our simulations and demonstrates that the number of simulations is roughly satisfactory for statistical analysis. Of course, the more slip ~~distribution~~distributions we use, the more comprehensive and stable the range we obtain.

In ~~Figure~~Fig. 5, the PTA distributions ~~at~~ for the stations in eastern Taiwan~~,~~ (red markers~~, are~~) have obviously higher values than ~~the~~those in western~~,~~ Taiwan (blue markers~~,~~) due to the specified location of the ~~source of~~ tsunami source. The shapes of the PTA distributions ~~at~~in eastern Taiwan ~~seem like log-normal distribution and at~~resemble lognormal distributions, while those in western~~, they seem like~~ Taiwan resemble normal ~~distribution~~distributions. We suppose that the attenuation of the wave propagation causes the ~~shape of log-normal distribution degenerating~~lognormal distributions to degenerate into normal ~~distribution.~~distributions. The ~~PTA~~PTAs produced by a uniform slip distribution are generally located in the middle of the PTA distributions. Both PTA values (i.e., the value of the PTA ~~values~~ from the uniform slip distribution and ~~the values of the PTA~~ those from the stochastic slip distribution models) decrease with the distance from the potential fault ~~because of the~~ due to attenuation of the wave propagation (~~Fig.~~Figure 5 ~~is~~shows the results for all stations, and Fig. 6 shows ~~station~~the results for stations 20 ~~to~~through 30 in ~~the~~ eastern Taiwan). However, some stations ~~are not perfectly following this, for instance, station~~, e.g., stations 17, 19, and 21 ~~which~~ , do not precisely follow this trend; this could be ~~affected by~~ the result of the coastal topography and the presence of an energy channel. From ~~Figure 3d,~~ Fig. 3d, in comparison with the adjacent coastline, station 21 ~~comparing with neighbor coast is~~is located exactly ~~at the location~~ where the wave energy gathers. In addition, ~~the~~ broad distributions are frequently ~~occur~~observed at promontories along the coastline and are caused by complex propagation path effects between the source region and the recording locations (Geist, 2002). There are many compound factors ~~to~~that affect the tsunami propagation and maximum wave height. Figure 6 presents the relation between the distance and wave height and ~~also~~ shows the PTA ~~distribution as Figure~~distributions following Fig. 5. The ~~distance is~~x-axis presents the shortest distance between the stations and fault plane. On the footwall side, ~~the station~~stations 20 and 22 ~~are outer island. They~~, which do not directly face the energy propagation path ~~directly~~ (Fig. 3f~~) so that the~~), are located on islands off the coast of Taiwan;

consequently, their PTA distributions are lower than ~~station~~those of stations 21 and 23~~;~~, even though the ~~distance~~distances from the potential fault are similar. On the hanging wall, station 29 is ~~far~~farther from ~~coast comparing~~ the coastline of Taiwan than other stations; however, because of the real location of the station and its numerical grid setting~~ so that the~~, its PTA distribution is lower than that of station 30 (Fig. 3b). The ranges of the PTA distributions converge with increasing distance on the both sides of the fault. Moreover, the PTA distributions and their average values roughly ~~appear~~exhibit a linear decrease with increasing distance except for stations 25 and 26. In contrast, these two stations in the near field~~, station 26 and 27. Moreover, the ranges of PTA distributions convergent with distance, too. On the other hand, the near field, station 26 and 27,~~ are directly affected by ~~seafloor deformation so that the PTA~~initial water elevation, and thus, the PTAs caused by uniform slip are quite low.

Although the seismic parameters have ~~defined~~ already been defined as constants in our experiment~~ and been held constants~~, there ~~exist~~exists an uncertainty ~~for~~in the PTA~~ rather than~~, which is not a constant value. ~~The~~Hence, the uniform case cannot provide ~~it~~this uncertainty, and thus, the PTA could be underestimated. ~~Results~~The results give specific PTA ranges, which ~~are~~represent the wave height uncertainties for the scenario of ~~the~~ earthquakes originating from the Ryukyu Trench. It is therefore necessary to consider the ~~effect by~~effects of a heterogeneous slip distribution ~~for a~~to comprehensively ~~assessing~~assess the tsunami hazard.

4 Discussion

4.1 Tsunami

Most ~~coast~~coastlines threatened by near~~-~~ field ~~tsunami is parallel the subduction zone like the coast~~tsunamis, such as the coasts of Chile, Japan and Indonesia~~. There~~, are ~~many~~parallel to the trench axis of the associated subduction zones. Many tsunami ~~event occurring these regions such as the 2010,~~events, including the Mw 8.8~~,~~ Chile earthquake in 2010 (Lay et al., 2010; Fritz et al., 2011), the ~~2011,~~ Mw 9.0~~,~~ Tohoku earthquake in 2011 (Goda et al., 2015; Goda and Song, 2016), the ~~2004,~~ Mw 9.1~~,~~ Sumatra earthquake in 2004 (Lay et al., 2005), and the ~~2010,~~ Mw 8.1~~,~~ Mentawai earthquake in 2010 (Satake et al., 2013~~).~~), have occurred along these regions. However, the potential rupture fault in this study along the southernmost Ryukyu subduction zone is perpendicular to the coast of Taiwan ~~island,~~ which directly affects the first ~~movement of~~ wave~~. On~~ motion. The first motion on the footwall~~, the first movement~~ is up~~, but~~; conversely~~, it is down. On~~ the first motion on the hanging wall is down. As a result, the coastline ~~backs~~retreats from the land to the sea ~~at~~as the first tsunami wave ~~that help~~approaches, allowing people ~~have more~~additional time to leave the seafront.

The effect ~~by~~of a heterogeneous slip distribution is important and necessary to consider for ~~the~~ near field ~~estimation~~estimations (Geist, 2002 and Ruiz et al., 2015). Figure 5 shows that the PTA distributions in the near field are broad, and they narrow with ~~distance~~ increasing distance from the potential fault. The uncertainty in the near field is higher than that in the far field. At ~~the~~ most of ~~east~~the eastern stations, the values of the average PTA approach uniform results, but ~~at station 25 and 26, their~~ the uniform slip results at stations 25 and 26 are close to the minimum PTA (Table 1~~.)~~.). Geist (2002) ~~presents~~presented the average and ~~extrema PTA in~~ extreme nearshore PTA calculated for 100 different slip distributions and ~~compares~~compared them with the uniform slip ~~result (Figure~~results (Fig. 6a in Geist~~,~~ (2002)). The range of the PTA also ~~narrows~~becomes narrower with ~~distance~~ increasing distance. The values ~~of~~from the uniform slip ~~result~~distribution and the average ~~of~~ PTA are similar, but ~~there are~~ some of the average values are close to the minimum PTA ~~around~~ between approximately 19 ºN ~~to~~and 19.5 ºN. ~~There is similar characteristic~~Similar characteristics of the average PTA and the results from the uniform ~~results~~ case are observed in different ~~region~~regions. The average PTA is equal to the uniform slip result in the nearshore region, but ~~that~~this could be caused by ~~the~~other factors (e.g.~~.~~., distance to the tsunami source, propagation path, initial water elevation, etc.) ~~to affect~~that shift the average PTA ~~to close to~~toward the minimum PTA.

~~There are four~~Four nuclear power plants (~~NPP)~~NPPs) are located on the island of Taiwan ~~island~~. According to the numerical results, we infer that the ~~PTA~~ mean ~~value of NPP4~~ PTA in the coastal area ~~is around~~of NPP4 ranges from approximately 2 to 3 m. ~~This~~The distribution at this plant may be ~~wilder~~wider than those at other nuclear power plants due to ~~the relative~~its position ~~of~~relative to the tsunami source. Moreover, NPP4 ~~locates a~~ is located on the shore of a bay with a curved shape ~~so that~~; the ~~extra~~ magnification effect ~~perhaps makes~~from the geometrical shape of the bay may serve to enhance the PTA ~~higher. The~~therein. NPP3 also ~~has~~exhibits this condition ~~and then~~insomuch that the energy ~~concentrates~~is concentrated at ~~this area~~the location of the plant (Fig. 3b, 3d and 3f). For the coastal areas around NPP1 and NPP2 ~~coastal area~~, the PTA distributions are between 1 and 2 m. The ~~coast~~coastlines of ~~this~~these two nuclear power plants ~~is facing~~slightly face the direction of tsunami ~~current slightly so that its PTA~~propagation, and thus, their PTAs should be higher than ~~neighbor coast~~those along adjacent coastlines (Fig. 3b, 3d and 3f). In general, under this scenario, the ~~coast of~~coastline at NPP4 has the largest threat. Although ~~the~~ NPP3 is far from ~~this~~the tsunami source, it ~~roughly~~ faces ~~1.5 m~~a wave height of approximately 1.5 m on average ~~and has~~with a ±0.~~5m uncertain~~5 m range~~.~~ of uncertainty. However, ~~the~~ NPP3 is ~~more close~~closer to the Manila subduction zone ~~which~~, and thus, it could be threatened by ~~the~~a tsunami originating from the Manila Trench. ~~The coast~~In contrast, the coastlines of NPP1 and NPP2 ~~is relative~~are relatively safe and ~~has less uncertainty for~~have fewer uncertainties with regard to the PTA.

The use of ~~a~~ heterogeneous slip ~~pattern~~patterns clearly delineates the range of possible waveforms and provides more information on latent uncertainties ~~of~~in the wave height. The 95% confidence intervals for the wave height from 100 sets ~~present~~ in each time series ~~and~~ provide us a specific range for the ~~motion~~amplitude of ~~sea level~~the tsunami wave (Fig. 4). According to these time series, we are aware of the periods of tsunami runup and runoff and can prepare ~~the~~ supporting policies to reduce ~~disaster.~~associated disasters. For example, a nuclear power plant ~~has the~~includes a trench ~~of water intake~~ from the ocean for ~~cooling~~ the intake of water to cool the reactor~~, and~~; thus, if the ~~motion of~~ sea level is too low to take ~~the~~in water, the temperature of the reactor will ~~be too high and then cause the~~ rise excessively, causing a nuclear disaster. Based on the results of simulations, we can estimate that how much water should be stored for tsunami runoff. This issue ~~is necessary to pay~~requires more attention in Taiwan because ~~there are~~ four ~~unclear~~nuclear power plants are located near the coast.

4.2 Stochastic slip model

The results of the tsunami simulations illustrate that the effect of the slip distribution on the rupture plane has ~~a~~ significant ~~effect~~effects on the wave propagation and wave height. The correctness of this slip distribution determines whether the wave height calculations represent a useful reference ~~or not~~. However, some parameters of the stochastic ~~model~~models could influence the synthetic slip distributions. For instance, the exponent of the slip spectrum ~~associates~~is associated with the roughness of the slip distribution. Higher exponential ~~value inhibits~~values inhibit the ~~power~~powers of high ~~wavenumber and leads it~~ wavenumbers, leading to smoother slip distributions; conversely, lower ~~value leads it~~ values lead to rougher~~.~~ slip distributions. In general, the *k*-square model needs to be followed. Furthermore, the interpolation of the slip distribution for a given geometry will affect the exponent of *k* (Tsai, 1997). Interpolation ~~make~~ will smooth the original pattern ~~smoother~~. The powers of short ~~wavenumber~~wavenumbers will be ~~depressing~~depressed and the powers of long ~~wavenumber~~wavenumbers will be ~~enhancing. Additionally~~enhanced. Moreover, the random spatial variability of the slip distribution is ~~more~~relatively critical. According to Lavallée and Archuleta (2003) and Lavallée et al~~.,~~. (2006), we ~~adopted~~adopt the truncated non-Gaussian distribution ~~as a~~for the spatial variability. ~~Truncation~~ This truncation limits the non-Gaussian distribution to a particular range. ~~The~~However, extreme truncation will cause the heavy-tailed characteristic of this distribution to become less pronounced or even disappear, ~~as in~~similar to a Gaussian distribution. ~~The~~In mathematics, the synthetic slip distribution is a filtering process ~~in mathematics so~~insomuch that the characteristics of a heavy-tailed ~~characteristic affects~~distribution affect the ~~extremum~~extrema of the slip distribution. The maximum slip will be greater as the truncated range increases~~. The~~, and the maximum slip may exceed reasonable values ~~as~~if the truncated range is ~~too~~excessively wide. Therefore, the parameters must be chosen carefully ~~in order~~ to match the observations acquired by inversion.

5 Conclusion

The maximum possible earthquake ~~scenario~~magnitude is M_w 8.15 with an average slip of 8.25 m in the southernmost portion of the Ryukyu Trench. ~~The 100~~One hundred slip distributions of the seismic rupture surface were generated by a stochastic slip model. The maximum slip range is between 20.17 ~~to~~and 37.97 m, and the average slip ~~all consists~~of each model is consistent with 8.25 m. ~~The~~A heterogeneous slip distribution induces variability in the tsunami wave heights and the associated paths of propagation. The simulated results demonstrate that ~~rupture~~the complexity of the rupture plane has a significant influence on the near field for local ~~tsunami~~tsunamis. The PTA distribution ~~provide~~provides a specific range for the wave height and ~~its occurring~~ the probability of occurrence in this scenario. These distributions and their average values ~~roughly appear a~~exhibit an approximately linear decrease with increasing distance. The ~~coast~~coastline, which is situated very close to or even atop the tsunami source ~~or even upon~~, is directly affected by the rupture slip~~.~~ distribution. Then, the range of the PTA distribution will converge with increasing distance ~~increasing~~ from the tsunami source. In this study, Hualien station, which is ~~upon~~located directly above the source, has the ~~wildest~~widest PTA interval (1.87-7.32 m) and the highest wave amplitude. The statistical summary reveals that this station, whose standard deviation is 1.63 ~~and~~m, which is larger than those of the other stations, has the largest uncertainty. However, the PTA caused by the uniform slip distribution is only 1.63 m, which is much lower~~,~~ and is even below the average (3.36 m) ~~in~~at this station. ~~It~~This finding implies that a simplified earthquake source cannot completely represent the tsunami amplitudes in reality. If we adopt a uniform slip distribution to assess tsunami ~~hazard, it~~hazards, those hazards will be critically underestimated. ~~The~~Furthermore, the variances of tsunami amplitudes~~, which have characteristically extreme variance,~~ are imperative for assessing tsunami hazards, and the quantitative ~~techniques~~technique employed is also important.

References

Aki, K.: Scaling law of seismic spectrum, J. Geophys. Res., 72, 1217-1231, 1967. doi:10.1029/JZ072i004p01217

Amante, C. and Eakins, B. W.: ETOPO1 1 arc-minute global relief model: procedures, data sources and analysis, US Department of Commerce, National Oceanic and Atmospheric Administration, National Environmental Satellite, Data, and Information Service, National Geophysical Data Center, Marine Geology and Geophysics Division Colorado, 2009. doi:10.7289/V5C8276M

Andrews, D. J.: A stochastic fault model: 1. Static case, J. Geophys. Res. Solid Earth, 85, 3867-3877, 1980. doi:10.1029/JB085iB07p03867

Burroughs, S. M. and Tebbens, S. F.: Power-law scaling and probabilistic forecasting of tsunami runup heights, Pure Appl. Geophys., 162, 331-342, 2005. doi:10.1007/s00024-004-2603-5

Chen, P.-F., Newman, A. V., Wu, T.-R., and Lin, C.-C.: Earthquake Probabilities and Energy Characteristics of Seismicity Offshore Southwest Taiwan, Terr. Atmos. Ocean. Sci., 19, 2008. doi:10.3319/TAO.2008.19.6.697(PT)

Cheng, S.-N., Shaw, C.-F., and Yeh, Y. T.: Reconstructing the 1867 Keelung Earthquake and Tsunami Based on Historical Documents, Terr. Atmos. Ocean. Sci., 27, 2016. doi:10.3319/TAO.2016.03.18.01(TEM)

Cornell, C. A.: Engineering seismic risk analysis, Bull. Seism. Soc. Am., 58, 1583-1606, 1968.

Davis, T. L. and Namson, J. S.: A Balanced Cross-Section of the 1994 Northridge Earthquake, Southern California, Nature, 372, 167-169, 1994. doi:10.1038/372167a0

Dean, R. G. and Dalrymple, R. A.: Water wave mechanics for engineers and scientists, World Scientific Publishing Co Inc, 1991. doi:10.1142/9789812385512_0004

Fowler, C. M. R.: The Solid Earth: An Introduction to Global Geophysics, Cambridge University Press, Cambridge. pp. 728. 2004. ISBN-10: 0521893070

Fritz, H. M., Petroff, C. M., Catalán, P. A., Cienfuegos, R., Winckler, P., Kalligeris, N., Weiss, R., Barrientos, S. E., Meneses, G., Valderas-Bermejo, C., Ebeling, C., Papadopoulos, A., Contreras, M., Almar, R., Dominguez, J. C., and Synolakis, C. E.: Field Survey of the 27 February 2010 Chile Tsunami, Pure Appl. Geophys., 168, 1989-2010, 2011. doi:10.1007/s00024-011-0283-5

Geist, E. L.: Complex earthquake rupture and local tsunamis, J. Geophys. Res. Solid Earth, 107, ESE 2-1-ESE 2-15, 2002. doi:10.1029/2000JB000139

Geist, E. L. and Dmowska, R.: Local Tsunamis and Distributed Slip at the Source. In: Seismogenic and Tsunamigenic Processes in Shallow Subduction Zones, Sauber, J. and Dmowska, R. (Eds.), Birkhäuser Basel, Basel, 1999. doi:10.1007/978-3-0348-8679-6_6

Geist, E. L. and Parsons, T.: Probabilistic Analysis of Tsunami Hazards*, Nat. Hazards, 37, 277-314, 2006. doi:10.1007/s11069-005-4646-z

Geist, E. L. and Parsons, T.: Assessment of source probabilities for potential tsunamis affecting the U.S. Atlantic coast, Mar. Geol., 264, 98-108, 2009. doi:10.1016/j.margeo.2008.08.005

Goda, K. and Song, J.: Uncertainty modeling and visualization for tsunami hazard and risk mapping: a case study for the 2011 Tohoku earthquake, Stoch Environ Res Risk Assess, 30, 2271-2285, 2016. doi:10.1007/s00477-015-1146-x

Goda, K., Yasuda, T., Mori, N., and Mai, P. M.: Variability of tsunami inundation footprints considering stochastic scenarios based on a single rupture model: Application to the 2011 Tohoku earthquake, J. Geophys. Res. Oceans, 120, 4552-4575, 2015. doi:10.1002/2014JC010626

Gutenberg, B. and Richter, C. F.: Frequency of earthquakes in California, Bull. Seism. Soc. Am., 34, 185-188, 1944.

Hanks, T. C. and Kanamori, H.: A moment magnitude scale, J. Geophys. Res. Solid Earth, 84, 2348-2350, 1979. doi:10.1029/JB084iB05p02348

Herrero, A. and Bernard, P.: A Kinematic Self-Similar Rupture Process for Earthquakes, Bull. Seism. Soc. Am., 84, 1216-1228, 1994.

Horikawa, K. and Shuto, N.: Tsunami disasters and protection measures in Japan, Tsunamis-Their Science and Engineering, Terra Scientific Publishing Company, 1983. 9-22, 1983.

Houston, J. R., Carver, R. D., and Markle, D. G.: Tsunami-Wave Elevation Frequency of Occurrence for the Hawaiian Islands, Army Engineer Waterways Experiment Station, Vicksburg, MS, 66 pp, 1977.

Hsu, Y.-J., Ando, M., Yu, S.-B., and Simons, M.: The potential for a great earthquake along the southernmost Ryukyu subduction zone, Geophys. Res. Lett., 39, n/a-n/a, 2012. doi:10.1029/2012GL052764

Hsu, Y.-J., Yu, S.-B., Simons, M., Kuo, L.-C., and Chen, H.-Y.: Interseismic crustal deformation in the Taiwan plate boundary zone revealed by GPS observations, seismicity, and earthquake focal mechanisms, Tectonophysics, 479, 4-18, 2009. doi:10.1016/j.tecto.2008.11.016

Ide, S., Baltay, A., and Beroza, G. C.: Shallow dynamic overshoot and energetic deep rupture in the 2011 Mw 9.0 Tohoku-Oki earthquake, Science, 332, 1426-1429, 2011. doi:10.1126/science.1207020

Kanamori, H. and Anderson, D. L.: Theoretical basis of some empirical relations in seismology, Bull. Seism. Soc. Am., 65, 1073-1095, 1975.

Lavallée, D. and Archuleta, R. J.: Stochastic modeling of slip spatial complexities for the 1979 Imperial Valley, California, earthquake, Geophys. Res. Lett., 30, 1245, 2003. doi:10.1029/2002GL015839

Lavallée, D., Liu, P., and Archuleta, R. J.: Stochastic model of heterogeneity in earthquake slip spatial distributions, Geophys. J. Int., 165, 622-640, 2006. doi:10.1111/j.1365-246X.2006.02943.x

Lay, T., Ammon, C. J., Kanamori, H., Koper, K. D., Sufri, O., and Hutko, A. R.: Teleseismic inversion for rupture process of the 27 February 2010 Chile (Mw 8.8) earthquake, Geophys. Res. Lett., 37, L13301, 2010. doi:10.1029/2010GL043379

Lay, T., Ammon, C. J., Kanamori, H., Xue, L., and Kim, M. J.: Possible large near-trench slip during the 2011 Mw 9.0 off the Pacific coast of Tohoku Earthquake, Earth Planets Space, 63, 32, 2011. doi:10.5047/eps.2011.05.033

Lay, T., Kanamori, H., Ammon, C. J., Nettles, M., Ward, S. N., Aster, R. C., Beck, S. L., Bilek, S. L., Brudzinski, M. R., Butler, R., DeShon, H. R., Ekström, G., Satake, K., and Sipkin, S.: The Great Sumatra-Andaman Earthquake of 26 December 2004, Science, 308, 1127-1133, 2005. doi:10.1126/science.1112250

Lay, T. and Wallace, T. C.: Modern global seismology, Academic press, 1995. ISBN: 9780127328706

Liu, P. L. F., Cho, Y. S., Yoon, S. B., and Seo, S. N.: Numerical Simulations of the 1960 Chilean Tsunami Propagation and Inundation at Hilo, Hawaii. In: Tsunami: Progress in Prediction, Disaster Prevention and Warning, Tsuchiya, Y. and Shuto, N. (Eds.), Springer Netherlands, Dordrecht, 1995. doi:10.1007/978-94-015-8565-1_7

Liu, P. L. F., Cho, Y. S., Briggs, M. J., Kanoglu, U., and Synolakis, C. E.: Runup of solitary waves on a circular Island, J. Fluid Mech., 302, 259-285, 1995. doi:10.1017/S0022112095004095

Ma, K.-F. and Lee, M.-F.: Simulation of historical tsunamis in the Taiwan region, Terr. Atmos. Ocean. Sci., 8, 13-30, 1997.

Ma, K.-F., Satake, K., and Kanamori, H.: The origin of the tsunami excited by the 1989 Loma Prieta Earthquake —Faulting or slumping?, Geophys. Res. Lett., 18, 637-640, 1991. doi:10.1029/91GL00818

Mimura, N., Yasuhara, K., Kawagoe, S., Yokoki, H., and Kazama, S.: Damage from the Great East Japan Earthquake and Tsunami - A quick report, Mitig Adapt Strat Gl, 16, 803-818, 2011. doi:10.1007/s11027-011-9297-7

Nakamura, M.: Fault model of the 1771 Yaeyama earthquake along the Ryukyu Trench estimated from the devastating tsunami, Geophys. Res. Lett., 36, n/a-n/a, 2009. doi:10.1029/2009GL039730

Okada, Y.: Surface deformation due to shear and tensile faults in a half-space, Bull. Seism. Soc. Am., 75, 1135-1154, 1985.

Okal, E. A.: Mode-wave equivalence and other asymptotic problems in tsunami theory, Phys. Earth Planet. Inter., 30, 1-11, 1982. doi:10.1016/0031-9201(82)90123-6

Piombo, A., Tallarico, A., and Dragoni, M.: Displacement, strain and stress fields due to shear and tensile dislocations in a viscoelastic half-space, Geophys. J. Int., 170, 1399-1417, 2007. doi:10.1111/j.1365-246X.2007.03283.x

Ruiz, J. A., Fuentes, M., Riquelme, S., Campos, J., and Cisternas, A.: Numerical simulation of tsunami runup in northern Chile based on non-uniform k −2 slip distributions, Nat. Hazards, 79, 1177-1198, 2015. doi:10.1007/s11069-015-1901-9

Satake, K., Nishimura, Y., Putra, P. S., Gusman, A. R., Sunendar, H., Fujii, Y., Tanioka, Y., Latief, H., and Yulianto, E.: Tsunami Source of the 2010 Mentawai, Indonesia Earthquake Inferred from Tsunami Field Survey and Waveform Modeling, Pure Appl. Geophys., 170, 1567-1582, 2013. doi:10.1007/s00024-012-0536-y

Sella, G. F., Dixon, T. H., and Mao, A.: REVEL: A model for Recent plate velocities from space geodesy, J. Geophys. Res. Solid Earth, 107, ETG 11-11-ETG 11-30, 2002. doi:10.1029/2000JB000033

Senior Seismic Hazard Analysis Committee (SSHAC): Recommendations for probabilistic seismic hazard analysis: guidance on uncertainty and use of experts, US Nuclear Regulatory Commission Washington, DC, 1997. doi:10.2172/479072

Seno, T., Stein, S., and Gripp, A. E.: A model for the motion of the Philippine Sea Plate consistent with NUVEL-1 and geological data, J. Geophys. Res. Solid Earth, 98, 17941-17948, 1993. doi:10.1029/93JB00782

Shao, G., Li, X., Ji, C., and Maeda, T.: Focal mechanism and slip history of the 2011 Mw 9.1 off the Pacific coast of Tohoku Earthquake, constrained with teleseismic body and surface waves, Earth Planets Space, 63, 9, 2011. doi:10.5047/eps.2011.06.028

Soloviev, S.: Recurrence of tsunamis in the Pacific, Tsunamis in the Pacific Ocean, 1970. 149-163, 1970.

Theunissen, T., Font, Y., Lallemand, S., and Liang, W.-T.: The largest instrumentally recorded earthquake in Taiwan: revised location and magnitude, and tectonic significance of the 1920 event, Geophys. J. Int., 183, 1119-1133, 2010. doi:10.1111/j.1365-246X.2010.04813.x

Tsai, C.-C. P.: Slip, Stress Drop and Ground Motion of Earthquakes: A View from the Perspective of Fractional Brownian Motion, Pure Appl. Geophys., 149, 689-706, 1997. doi:10.1007/s000240050047

Tsai, Y.-B.: A study of disastrous earthquakes in Taiwan, 1683–1895, Bull. Inst. Earth Sci., Acad. Sin. 5, 1-44, 1985

Wang, X.: User manual for COMCOT version 1.7 (first draft). Cornel University, 65., 2009.

Wang, X. M. and Liu, P. L. F.: A numerical investigation of Boumerdes-Zemmouri (Algeria) earthquake and tsunami, CMES Comput. Model. Eng. Sci., 10, 171-183, 2005. doi:10.3970/cmes.2005.010.171

Wang, X. and Liu, P. L. F.: An analysis of 2004 Sumatra earthquake fault plane mechanisms and Indian Ocean tsunami, J. Hydraul. Res., 44, 147-154, 2006. doi:10.1080/00221686.2006.9521671

Wang, X. and Liu, P. L. F.: Numerical simulations of the 2004 Indian Ocean tsunamis — coastal effects, J. Earthquake and Tsunami, 01, 273-297, 2007. doi:10.1142/s179343110700016x

Wang, Y.-J., Chan, C.-H., Lee, Y.-T., Ma, K.-F., Shyu, J., Rau, R.-J., and Cheng, C.-T.: Probabilistic seismic hazard assessment for Taiwan, Terr. Atmos. Ocean. Sci., 27, 2016. doi:10.3319/TAO.2016.05.03.01(TEM)

Wu, T.-R., Chen, P.-F., Tsai, W.-T., and Chen, G.-Y.: Numerical Study on Tsunamis Excited by 2006 Pingtung Earthquake Doublet, Terr. Atmos. Ocean. Sci., 19, 705-715, 2008. doi:10.3319/TAO.2008.19.6.705(PT)

Wu, Y.-H., Chen, C.-C., Turcotte, D. L., and Rundle, J. B.: Quantifying the seismicity on Taiwan, Geophys. J. Int., 194, 465-469, 2013. doi:10.1093/gji/ggt101

Yu, N.-T., Yen, J.-Y., Chen, W.-S., Yen, I. C., and Liu, J.-H.: Geological records of western Pacific tsunamis in northern Taiwan: AD 1867 and earlier event deposits, Mar. Geol., 372, 1-16, 2016. doi:10.1016/j.margeo.2015.11.010

Yu, S.-B., Chen, H.-Y., and Kuo, L.-C.: Velocity field of GPS stations in the Taiwan area, Tectonophysics, 274, 41-59, 1997. doi:10.1016/S0040-1951(96)00297-1

Yue, H. and Lay, T.: Inversion of high-rate (1 sps) GPS data for rupture process of the 11 March 2011 Tohoku earthquake (Mw 9.1), Geophys. Res. Lett., 38, L00G09, 2011. doi:10.1029/2011GL048700

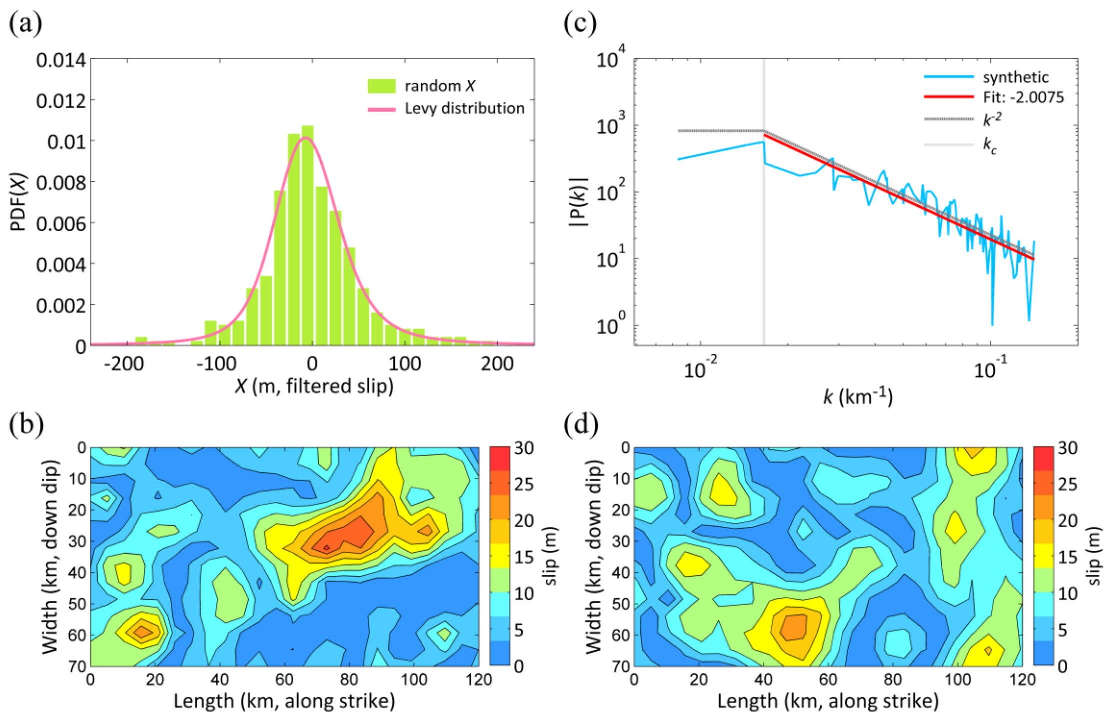

~~Fig.~~

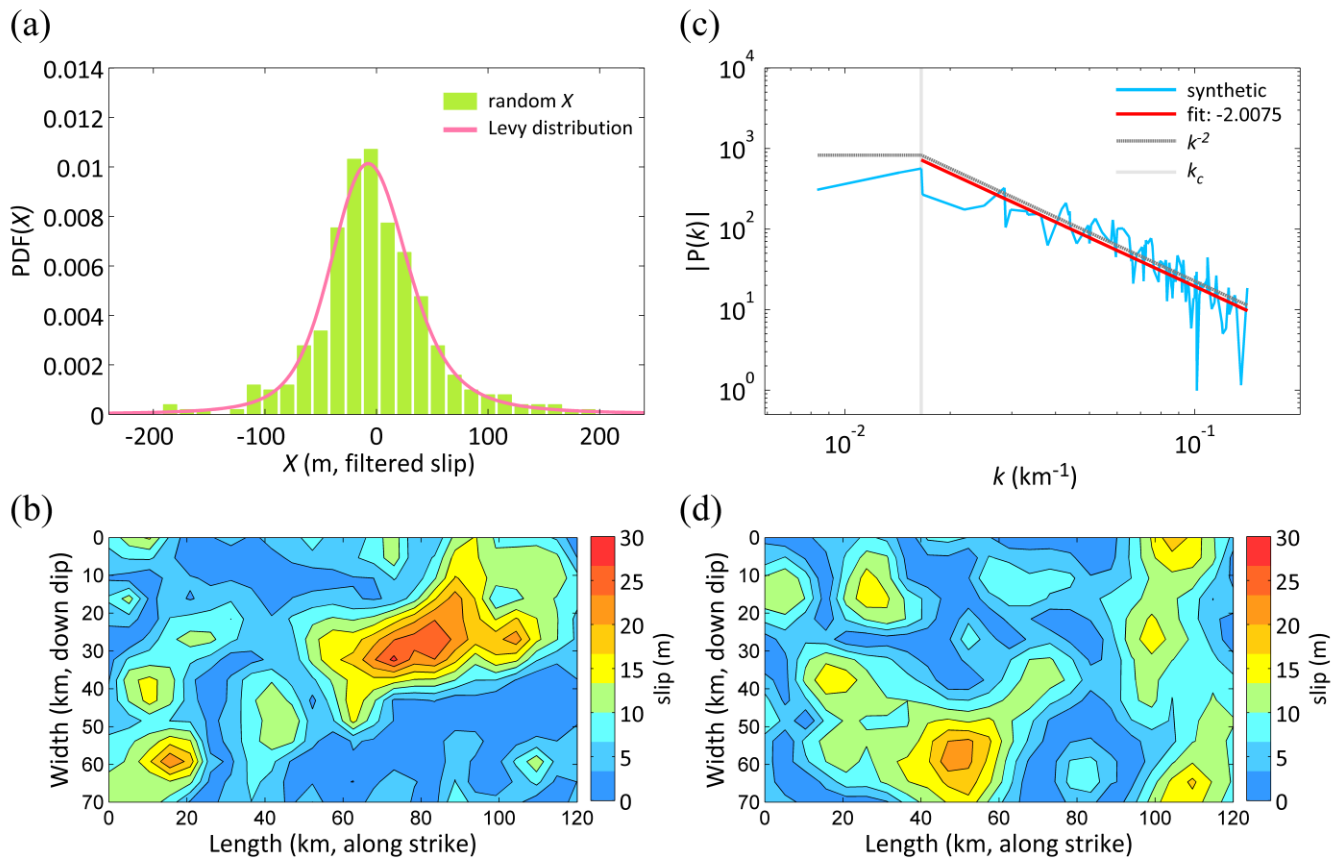

Figure 1~~.~~: (a) The ~~spatial~~spatially random variable: truncated Lèvy distribution. The Lèvy parameters obtained from the Northridge earthquake were taken from Lavallée et al (2006). (b) A stochastic slip distribution is generated ~~from~~by filtering the spatial random variable *X*~~,~~ in Fig. 1a. This slip pattern produces the highest maximum wave amplitude at Hualien station. (c) ~~Slip~~The slip spectrum is calculated from Fig. 1b. This slip spectrum decays with an exponent of -2 ~~and~~according to a characteristic ~~of~~ corner radial wavenumber. ~~It~~This verifies that the synthetic slip distribution is identical ~~with~~to the *k*-square model and the condition of the rupture dimension. (d) This stochastic slip distribution produces the lowest maximum wave amplitude at Hualien station.

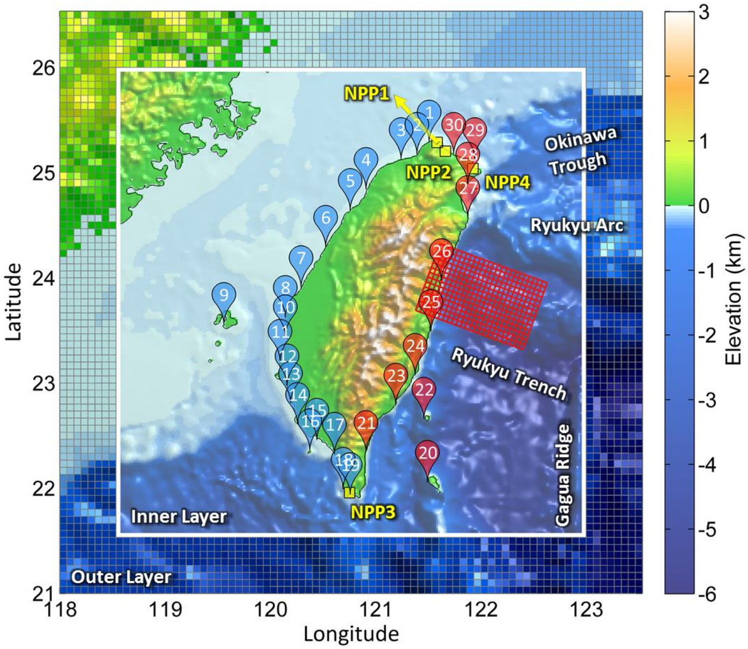

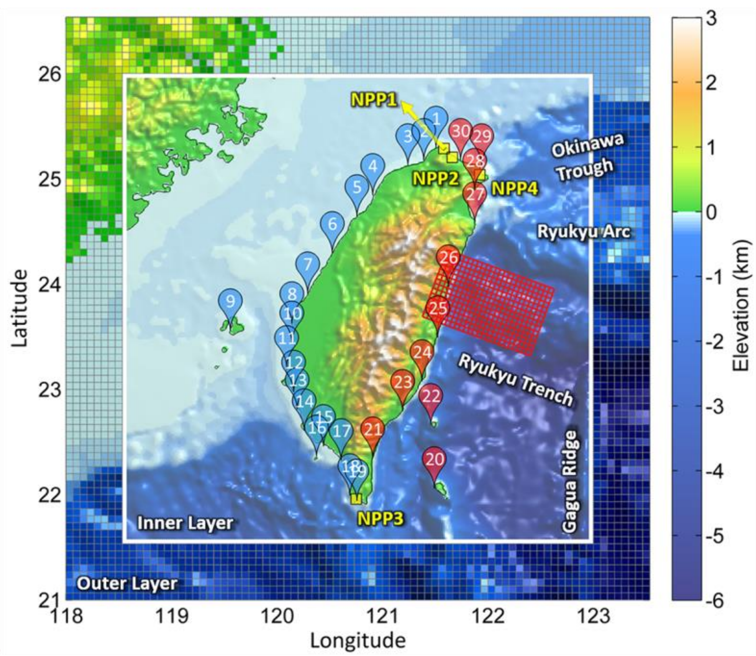

~~Fig.~~

Figure 2~~.~~: The map of Taiwan ~~presents~~shows the fault model and ~~recoding~~recording stations used in this study. The bathymetry is divided into 2 ~~layer for~~layers with different resolutions. The resolution of the outer layer is 4 minutes, and the resolution of the inner layer ~~of the white box~~ is 1 minute. The red grid denotes the potential fault model (5×5 km^2~~). Pins~~ grid size). The pins represent 30 tidal gauges of the CWB. The red and blue colors indicate stations on the ~~east~~eastern and ~~west~~western sides of Taiwan, respectively~~.~~ ~~Yellow~~, and the yellow squares represent the sites of ~~the~~ nuclear power plants.

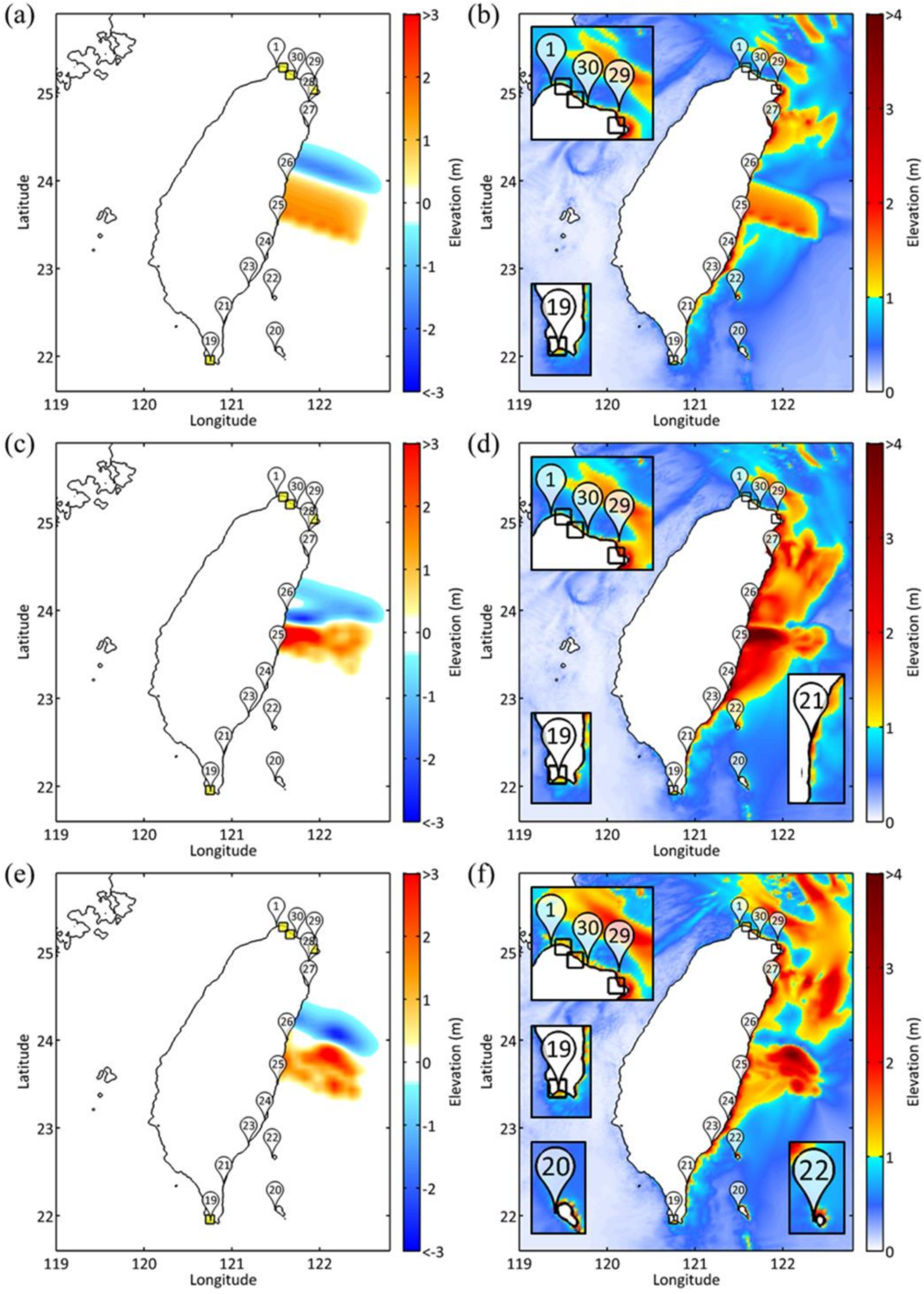

~~Fig.~~ Figure 3~~.~~: (a), (c) and (e) are the initial water ~~elevation~~ elevations, and ~~colorbar represents~~ the color bars represent the elevation of the initial water surface. (b), (d) and (f) are the maximum free-surface elevation~~,~~ (i.e., the distribution of the energy path~~,~~), and ~~colorbar represents~~ the color bars represent the elevation of the maximum free-surface. (a) and (b) displays the results ~~from~~ with a uniform slip distribution. (c) and (d) displays the results from Fig. 1b. (e) and (f) displays the results from Fig. 1d. ~~In fundamental,~~ The

seafloor ~~dominants~~ elevation fundamentally dominates the tsunami propagation, but the slip distribution also has a strong influence. In (a, c and e), yellow squares represent ~~nuclear power plants~~NPPs; in (b, d and f), ~~they~~the NPPs are represented by open squares.

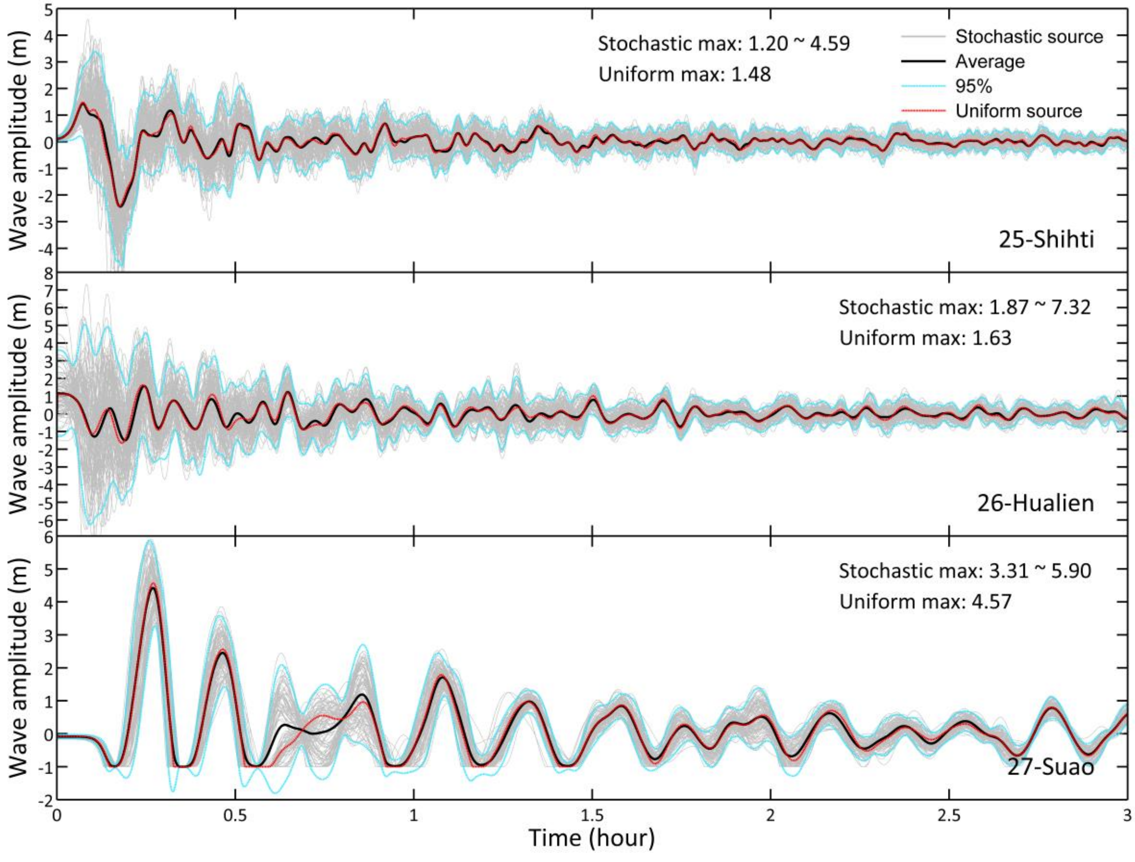

~~Fig.~~

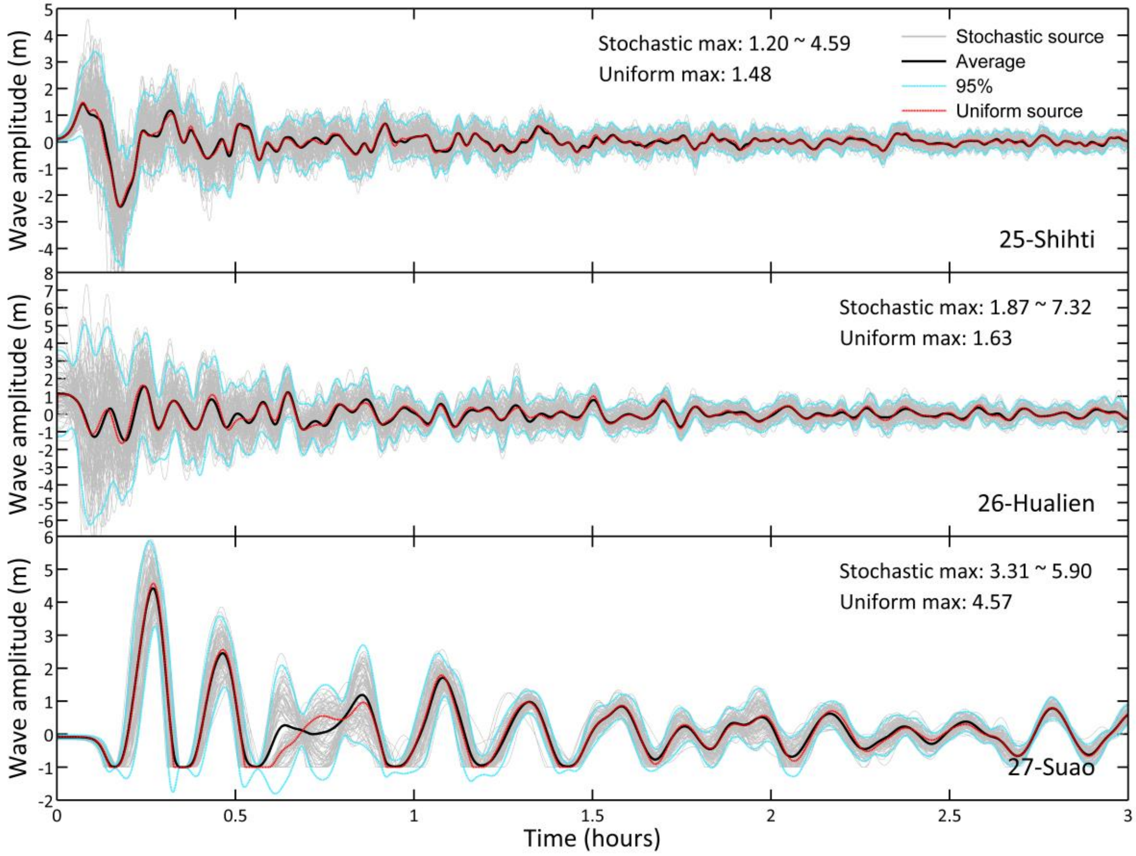

Figure 4~~.~~: The time series of the wave heights recorded at ~~station~~stations 25 (Shihti), 26 (Hualien) and 27 (Suao). Gray lines represent the time series of 100 different slip distributions; black lines represent the averages of the gray lines; blue lines represent the 95% confidence intervals; and red lines are the time series produced using uniform slip ~~distributions.~~distribution. Parts of the wave heights ~~on~~at station 27 are lower than the water depths, and thus, these curves have been truncated.

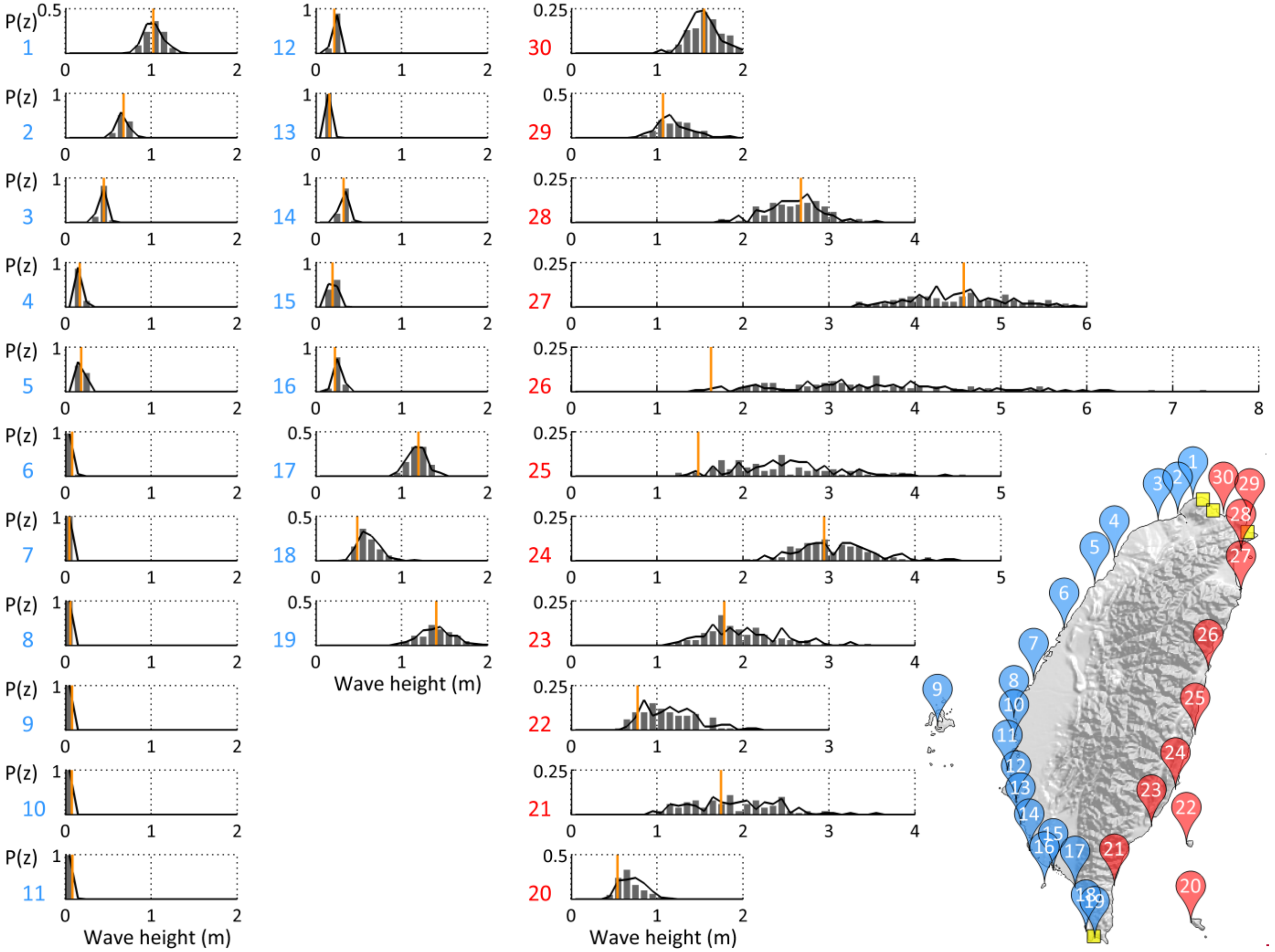

P(z)
Wave height (m)
Wave height (m)
Wave height (m)

~~Fig.~~

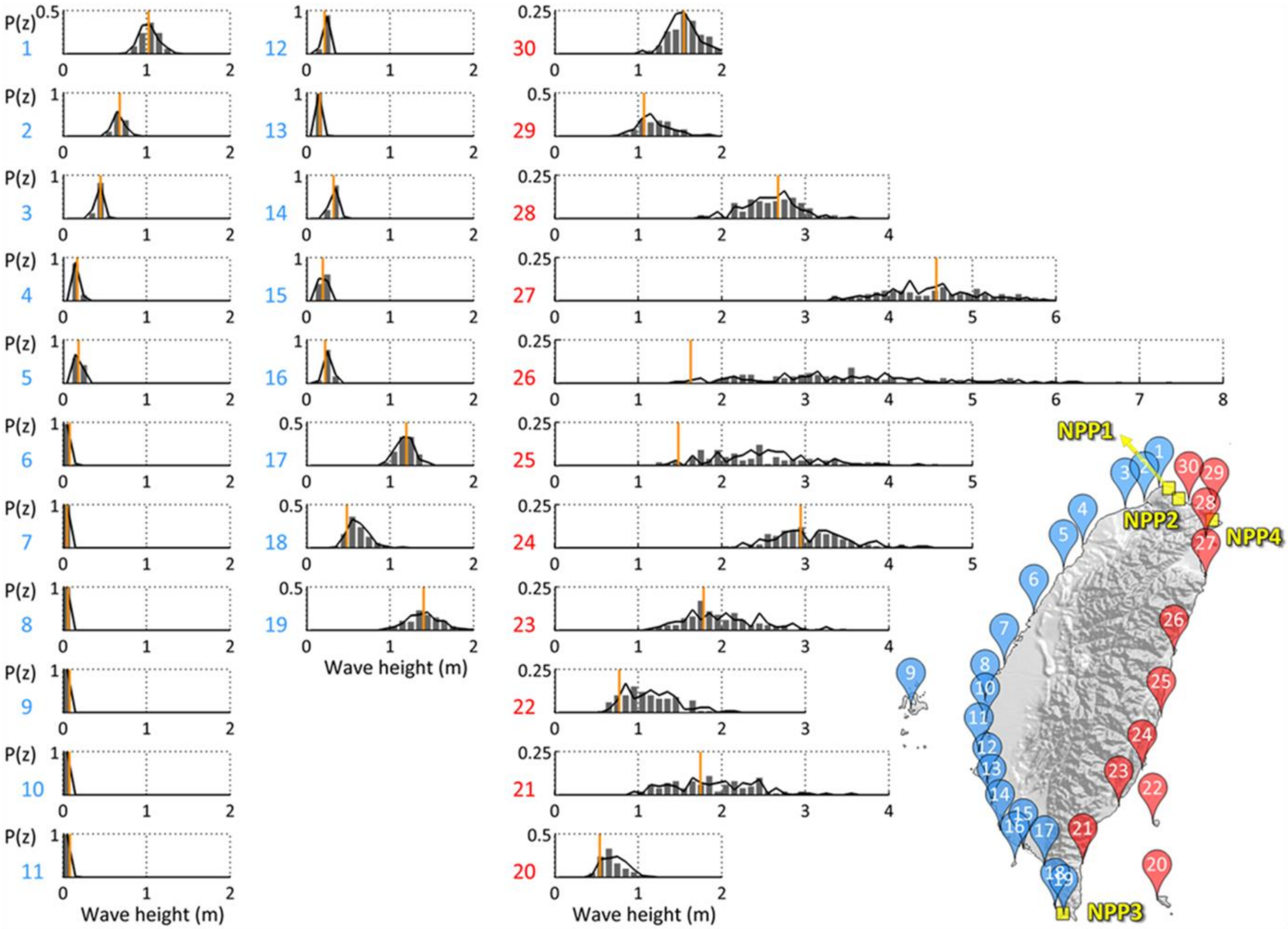

Figure 5~~.~~: The probabilities of the PTA along the coast of Taiwan (blue: stations 1~19, red: stations 20~30). The histograms display the ~~PTA~~PTAs derived from 100 different slip simulations. The black lines represent the results from another 100 simulations, and the orange lines represent the PTA obtained using a uniform slip distribution. The PTA probability distribution ~~give~~gives a clear PTA range and its occurring probability. The map of Taiwan shows the station locations and the sites of four NPPs (yellow squares).

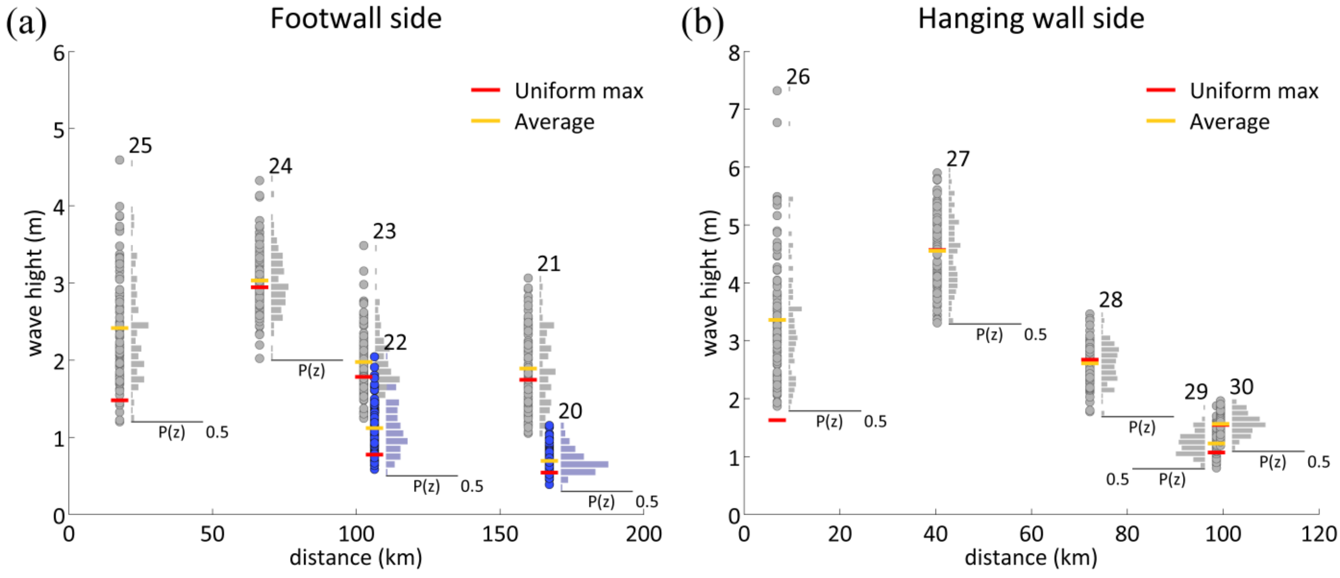

~~Fig.~~

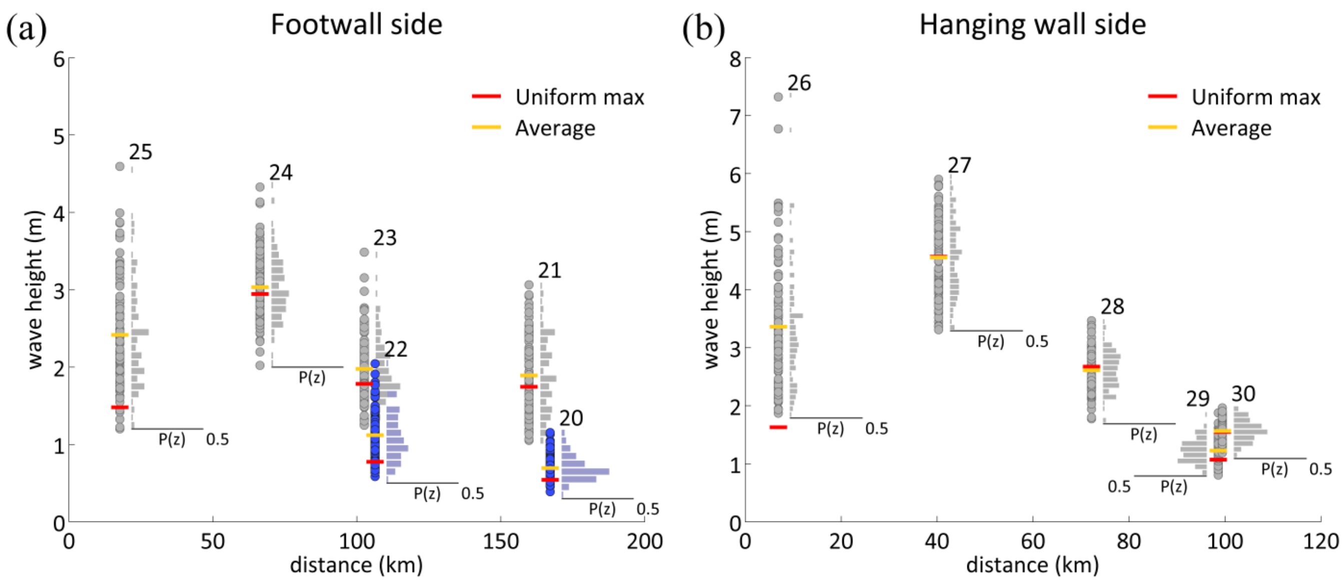

Figure 6~~.~~: The relation between the distance and wave height for stations ~~from~~ 20 ~~to~~through 30 in ~~the~~ eastern Taiwan. (a) is the station on the footwall side. ~~Station~~Stations 20 and 22~~,~~ (blue color~~,~~) are ~~out~~off the shoreline of Taiwan ~~island~~. (b) ~~is~~represents the stations on the hanging wall side. Both sides roughly ~~appear~~exhibit a linear decay and range of uncertainty ~~range~~ converging with ~~distance~~ increasing distance for the tsunami amplitude. Red bars show the PTA of the uniform slip distribution, and yellow bars show the average of the ~~PTA~~PTAs from the stochastic slip models.

Table 1~~. This table lists the~~: The maximum, minimum, ~~standard deviation~~ and average wave heights with their standard deviations for the PTA probability distributions (in ~~meter. It also lists~~meters) with the maximum wave heights from the uniform slip model. The water depths at the stations in the computational mesh are also included.

#	Station	Lon.	Lat.	Min [m]	Max [m]	σ [m]	Avg. [m]	Max [m] (uniform slip)	Water depth [m]
1	Linshanbi	121.5106	25.2844	0.80	1.32	0.108	1.04	1.02	4.00
2	Danshuei	121.4019	25.1844	0.55	0.83	0.061	0.68	0.68	4.00
3	Jhuwei	121.2353	25.1200	0.33	0.52	0.039	0.44	0.45	1.75
4	Hsinchu	120.9122	24.8503	0.13	0.24	0.025	0.17	0.17	3.50
5	Waipu	120.7717	24.6514	0.15	0.26	0.020	0.20	0.19	0.50
6	Taichung Port	120.5250	24.2917	0.07	0.11	0.009	0.08	0.08	0.00
7	Fanyuan	120.2972	23.9147	0.04	0.06	0.004	0.05	0.05	1.00
8	Bozihliao	120.1417	23.6250	0.05	0.07	0.004	0.06	0.06	0.00
9	Penghu	119.5669	23.5636	0.07	0.09	0.005	0.08	0.08	1.00
10	Dongshih	120.1417	23.4417	0.06	0.09	0.005	0.08	0.08	1.00
11	Jiangjyun	120.1000	23.2181	0.06	0.10	0.007	0.09	0.09	0.00
12	Anping	120.1583	22.9750	0.15	0.26	0.018	0.22	0.22	0.00
13	Yongan	120.1917	22.8083	0.11	0.20	0.016	0.16	0.16	5.25
14	Kaohsiung	120.2883	22.6144	0.23	0.43	0.039	0.33	0.33	2.00
15	Donggang	120.4417	22.4583	0.15	0.28	0.026	0.21	0.20	7.25
16	Siaoliouciou	120.3750	22.3583	0.17	0.40	0.046	0.26	0.22	12.75
17	Jiahe	120.6083	22.3250	0.90	1.44	0.098	1.19	1.20	4.00
18	Syunguangzuei	120.6917	21.9917	0.33	0.96	0.124	0.61	0.49	64.25
19	Houbihu	120.7583	21.9417	0.90	1.96	0.197	1.41	1.40	15.50
20	Lanyu	121.4917	22.0583	0.39	1.15	0.155	0.69	0.54	347.50
21	Dawu	120.8972	22.3375	1.05	3.06	0.487	1.89	1.74	31.75
22	Lyudao	121.4647	22.6622	0.58	2.04	0.316	1.12	0.78	146.00
23	Fugang	121.1917	22.7917	1.25	3.48	0.409	1.98	1.78	24.00
24	Chenggong	121.3767	23.0889	2.02	4.33	0.416	3.03	2.94	32.50
25	Shihti	121.5250	23.4917	1.20	4.59	0.680	2.42	1.48	142.75
26	Hualien	121.6231	23.9803	1.87	7.32	1.024	3.36	1.63	37.00
27	Suao	121.8686	24.5856	3.31	5.90	0.641	4.55	4.57	1.00
28	Gengfang	121.8619	24.9072	1.78	3.47	0.337	2.61	2.67	24.00
29	Longdong	121.9417	25.1250	0.80	1.88	0.202	1.23	1.07	60.75

30	Keelung	121.7417	25.1750	1.19	1.96	0.183	1.57	1.55	15.50